Genetic interactions between the chromosome axis-associated protein Hop1 and homologous recombination determinants in *Schizosaccharomyces pombe*

Simon David Brown[1,2], Olga Dorota Jarosinska[1], and Alexander Lorenz[1,*]

[1]Institute of Medical Sciences (IMS), University of Aberdeen, Aberdeen AB25 2ZD, United Kingdom

[2]Present address: MRC Institute of Genetics & Molecular Medicine, University of Edinburgh, Edinburgh EH4 2XU, United Kingdom

Key words: *Schizosaccharomyces pombe*, meiosis, homologous recombination, chromosome axis, Hop1

*Correspondence should be addressed to:

Alexander Lorenz

Institute of Medical Sciences (IMS)

University of Aberdeen

Foresterhill

Aberdeen AB25 2ZD

United Kingdom

Phone: +44 1224 437323

E-mail: a.lorenz@abdn.ac.uk

Alexander Lorenz ORCID 0000-0003-1925-3713

Abstract

Hop1 is a component of the meiosis-specific chromosome axis and belongs to the evolutionarily conserved family of HORMA domain proteins. Hop1 and its orthologs in higher eukaryotes are a major factor in promoting double-strand DNA break formation and inter-homolog recombination. In budding yeast and mammals they are also involved in a meiotic checkpoint kinase cascade monitoring the completion of double-strand DNA break repair. We used the fission yeast, *Schizosaccharomyces pombe*, which lacks a canonical synaptonemal complex to test whether Hop1 has a role beyond supporting the generation of double-strand DNA breaks and facilitating inter-homolog recombination events. We determined how mutants of homologous recombination factors genetically interact with *hop1*, studied the role(s) of the HORMA domain of Hop1, and characterized a bio-informatically predicted interactor of Hop1, Aho1 (SPAC688.03c). Our observations indicate that in fission yeast, Hop1 does require its HORMA domain to support wild-type levels of meiotic recombination and localization to meiotic chromatin. Furthermore, we show that *hop1*Δ only weakly interacts genetically with mutants of homologous recombination factors, and in fission yeast likely has no major role beyond break formation and promoting inter-homolog events. We speculate that after the evolutionary loss of the synaptonemal complex, Hop1 likely has become less important for modulating recombination outcome during meiosis in fission yeast, and that this led to a concurrent rewiring of genetic pathways controlling meiotic recombination.

Introduction

Chromosomes of diploid organisms are present in two sets, each derived from one of the parents. To reproduce sexually, this genetic material is halved exactly to produce haploid cells that contain only one chromosome set, the gametes. During fertilization, two gametes from different sexes fuse to form a zygote, re-establishing a double chromosome set. A specialized kind of cell division, called meiosis, is employed to halve the genetic material. In meiosis, one round of chromosome duplication is followed by two rounds of chromosome segregation. Remarkably, correct segregation of chromosomes in meiosis requires formation of double-strand DNA breaks (DSBs) by the conserved transesterase Spo11 (Lam and Keeney 2015), followed by repair through homologous recombination. Homologous recombination, in combination with sister chromatid cohesion, establishes physical connections (chiasmata) between maternal and paternal chromosomes that guide their proper segregation, and promotes reciprocal exchange (crossovers) of maternal and paternal genetic information (Hunter 2015). Careful regulation of this complex process is imperative to ensure the required number of physical links between the correct partner chromosomes, and that unrepaired DNA breaks are mended (Lam and Keeney 2015; Hunter 2015).

The repair of the Spo11-induced DSBs is started by DNA resection. During the initial step of DNA resection Spo11, which is covalently linked to the DNA ends, is endonucleolytically removed by the Mre11-Rad50-Nbs1 (Mre11-Rad50-Xrs2 in *Saccharomyces cerevisiae*) complex in cooperation with Ctp1 (Sae2 in *S. cerevisiae*) (Neale et al. 2005; Hartsuiker et al. 2009). Long-range resection then exposes substantial 3’ tails which are used to invade homologous template DNA on the homologous chromosome or the sister chromatid (strand exchange) to mend the DSB by recombination (reviewed in Mimitou and

73 Symington 2011; Hunter 2015; Lorenz 2017). Key factors for the strand exchange process in
74 meiosis are the RecA-type recombinases Rad51 and Dmc1 (Shinohara et al. 1997; Grishchuk
75 and Kohli 2003) supported by their mediators Rad55-Rad57, Swi5-Sfr1, and Rlp1-Rdl1-Sws1
76 (SHU complex in *S. cerevisiae*) (Tsutsui et al. 2001; Grishchuk and Kohli 2003; Akamatsu et al.
77 2003; Martín et al. 2006; Sasanuma et al. 2013; Hong et al. 2013; Lorenz et al. 2014). These
78 Rad51/Dmc1-mediators are important for generating and stabilizing Rad51/Dmc1 coated
79 nucleoprotein filaments which then invade homologous template DNA (Sung 1997; Haruta et
80 al. 2006). The DNA on the homologous chromosome (or sister chromatid) being invaded is
81 opened as a displacement loop (D-loop) which can then be extended by DNA synthesis using
82 the invading sequence as primer (reviewed in Brown and Bishop 2014). The way in which D-
83 loops or recombination intermediates derived from it are processed, determines whether
84 repair will occur as a crossover (CO) or a non-CO, and Rad51/Dmc1-mediators play an
85 important role in this (reviewed in Brown and Bishop 2014; Hunter 2015; Lorenz 2017).

86 In fission yeast processing of most meiotic recombination intermediates into COs and
87 some non-COs depends on the structure-selective endonuclease Mus81-Eme1, the lack of
88 which results in meiotic catastrophe and strongly reduced spore viability (Osman et al. 2003;
89 Smith et al. 2003). Additionally, a sizeable fraction of non-COs is produced by the action of
90 the FANCM-ortholog Fml1, a DEAD/DEAH-box DNA helicase, and it has been shown that
91 Mus81-Eme1 and Fml1 work in parallel to process meiotic recombination intermediates
92 (Lorenz et al. 2012). In a wild-type situation Fml1 action seems to be curtailed by
93 Rad51/Dmc1-mediators, because weakening the strand exchange reaction by removing any
94 Rad51/Dmc1-mediator in a *mus81*Δ background ameliorates the strong spore viability defect
95 of *mus81*Δ without restoring CO formation; this rescue depends on the presence of Fml1
96 (Lorenz et al. 2012, 2014).

97 To facilitate the generation of DSBs and their correct repair during meiosis,
98 chromosomes undergo a progression of changes starting with the establishment of meiosis-
99 specific chromosome axes and, in most organisms, culminating in the formation of the
100 synaptonemal complex – an elaborate proteinaceous structure (reviewed in Cahoon and
101 Hawley 2016). Components of the synaptonemal complex seem to be critical for controlling
102 several aspects of meiotic chromosome metabolism, from pairing of homologous
103 chromosomes, to initiation of recombination and maturation of the physical interactions
104 between the homologous chromosomes (reviewed in Cahoon and Hawley 2016; Gray and
105 Cohen 2016). However, some organisms have overcome the necessity for a fully-fledged
106 synaptonemal complex and perform meiosis with a simplified version of it (reviewed in Loidl
107 2016). The fission yeast *Schizosaccharomyces pombe* is the best-studied organism executing
108 meiosis without a canonical synaptonemal complex (reviewed in Loidl 2006).

109 Despite lacking a synaptonemal complex, fission yeast meiotic chromosomes
110 assemble axes, called linear elements (Olson et al. 1978; Bähler et al. 1993; Molnar 2003),
111 consisting of proteins which are evolutionarily related to axial/lateral elements of the
112 synaptonemal complex (Lorenz et al. 2004), and building upon the existing mitotic
113 chromosome axis organization (reviewed in Ding et al. 2016; Iwasaki and Noma 2016). One
114 of these components is Hop1 which, in contrast to other meiotic chromosome axis factors, is
115 conserved on the protein sequence level with homologs from yeast to man (Lorenz et al.
116 2004; Rosenberg and Corbett 2015). In both *S. cerevisiae* and *Sz. pombe*, Hop1 localizes to
117 the meiosis-specific chromosome axis (Hollingsworth et al. 1990; Smith and Roeder 1997;
118 Lorenz et al. 2004), and deletion of *HOP1/hop1*$^{+}$ causes a decrease in meiotic recombination
119 and homologous chromosome pairing (Hollingsworth and Byers 1989; Loidl et al. 1994;
120 Latypov et al. 2010). Hop1 is characterized by a conserved N-terminal HORMA (Hop1-Rev7-

121 Mad2) domain (Aravind and Koonin 1998) (Fig. 1a) and is the founding member of the
122 meiotic HORMA domain (HORMAD) family proteins. In contrast to yeasts which contain only
123 one meiotic HORMAD (Hop1), higher eukaryotes contain multiple paralogs of meiotic
124 HORMADs: These include HIM-3, HTP-1, HTP-2, and HTP-3 in *C. elegans*; ASY1 and ASY2 in
125 *Arabidopsis*; and HORMAD1 and HORMAD2 in mammals (Zetka et al. 1999; Caryl et al. 2000;
126 Couteau and Zetka 2005; Martinez-Perez and Villeneuve 2005; Goodyer et al. 2008; Fukuda
127 et al. 2010). In fungi, plants, and mammals the HORMA domain is followed by several [S/T]Q
128 residues representing potential Tel1/ATM-Rad3/Mec1/ATR phosphorylation sites, which
129 enable meiotic HORMADs to act as structural adaptors for a meiotic checkpoint kinase
130 cascade (Sanchez-Moran et al. 2007; Carballo et al. 2008; Daniel et al. 2011; Kogo et al.
131 2012; Osman et al. 2018) (Fig. 1a). Fungal Hop1 proteins also contain a centrally located CxxC
132 Zn-finger motif (Hollingsworth et al. 1990) (Fig. 1a) which has been demonstrated to be
133 important for *in vitro* DNA-binding of *S. cerevisiae* Hop1 (Tripathi et al. 2007). Despite its *in*
134 *vitro* DNA-binding capabilities, Hop1 requires the presence of Rec10 (Red1 in *S. cerevisiae*) to
135 localize to chromosome axes *in vivo* (Smith and Roeder 1997; Lorenz et al. 2004); indeed,
136 Hop1 and Rec10/Red1 have been shown to physically interact with each other (de los Santos
137 and Hollingsworth 1999; Spirek et al. 2010). Rec10 in turn is recruited to chromosome axes
138 by the meiosis-specific cohesin subunit Rec11 upon phosphorylation by casein kinase 1
139 (Phadnis et al. 2015; Sakuno and Watanabe 2015).

140 Here, we investigate genetic interactions of *hop1* with meiotic recombination
141 determinants in fission yeast to test whether *hop1* has (a) role(s) beyond its established
142 function in promoting DSB formation (Latypov et al. 2010). Genetic interactions with factors
143 important for recombination intermediate processing (*mus81* and *fml1*) suggested a
144 potential, likely indirect, role for Hop1 in the strand exchange process. However, subsequent

145 epistasis analysis with the strand exchange factor *dmc1* and Rad51/Dmc1-mediators (*rad55*,
146 *sfr1,* and *rlp1*) did not support the hypothesized separate function of Hop1 in strand
147 exchange. Furthermore, we also show that the HORMA domain is required for wild-type
148 levels of meiotic recombination, and for localization to meiotic chromatin in *Sz. pombe*.
149 Implications of the evolutionary differences regarding meiotic HORMAD proteins and their
150 interactions are discussed.
151

152 **Material and methods**

153 ***Sz. pombe* and *E. coli* culture conditions**

154 *E. coli* strains were grown on LB and SOC media – where appropriate containing 100 µg/ml
155 Ampicillin (Sambrook and Russell 2000). Competent cells of *E. coli* strains NEB10®-beta (New
156 England BioLabs Inc., Ipswich, MA, USA), and XL1-blue (Agilent Technologies, Santa Clara, CA,
157 USA) were transformed following the protocols provided by the manufacturers.

158 *Sz. pombe* strains used for this study are listed in Supplementary Table S1. Yeast cells
159 were cultured on yeast extract (YE), yeast nitrogen base glutamate (YNG) and Edinburgh
160 minimal media with glutamate as nitrogen source (EMMG) agar plates containing the
161 required supplements (concentration 250 mg/l on YE, 75 mg/l on YNG and EMMG). Crosses
162 were performed on malt extract (ME) agar containing the required supplements at a final
163 concentration of 50 mg/l, unless strains to be crossed contained plasmids, in which case they
164 were sporulated on sporulation agar with supplements (SPAS) plates with the necessary
165 supplements at 50 mg/l to maintain selection for the plasmids (Smith 2009; Sabatinos and
166 Forsburg 2010). Transformation of yeast strains was done using a standard lithium-acetate
167 procedure (Keeney and Boeke 1994) with the modifications described in Brown and Lorenz
168 (2016).

169 To obtain meiotic *Sz. pombe* cells for chromatin spreading and cDNA preparation
170 meiotic time-courses were executed according to a published protocol (Loidl and Lorenz
171 2009).
172
173 **Yeast strain and plasmid construction**
174 For specifics of strain and plasmid construction, please refer to Supplementary Materials.
175 Construction of the *kanMX6*-marked *hop1Δ-1* allele (Latypov et al. 2010) and the
176 kanMX6-marked *mug20*$^{+}$*-GFP* (Estreicher et al. 2012) have been described previously. The
177 *natMX6*-marked *hop1Δ-25* was derived from *hop1Δ-1* using an established marker swap
178 protocol (Sato et al. 2005; Lorenz 2015).
179 To produce *hop1*-alleles expressing a particular splice variant or the *hop1-ΔHORMAD*
180 mutant, we first partially deleted *hop1* retaining the coding sequence directly upstream of
181 the first and directly downstream of the last intron using a *ura4* marker (Grimm et al. 1988).
182 The resulting strain carrying the *hop1-3* allele (UoA725) was subsequently transformed with
183 the cDNA of one of the two splice variants or a *hop1-ΔHORMAD* construct; candidate strains
184 were selected by resistance to FOA (5-fluoroorotic acid) and then subjected to further
185 testing.
186 Epitope-tagging of Hop1 with 13myc was achieved by cloning a transformation
187 cassette into pFA6a-*13myc-kanMX6* (Bähler et al. 1998) with sequences from the 3' end and
188 downstream flanking region of the *hop1* coding sequence. This transformation cassette was
189 amplified by PCR and transformed into strains UoA746, UoA868, and UoA938.
190 A deletion cassette for *aho1* was constructed by cloning flanking sequences of
191 *SPAC688.03c* into pAG25 up- and downstream of the *natMX4* marker (Goldstein and

192 McCusker 1999). The resulting plasmid (pALo116) was linearized by a restriction digest and
193 transformed into the standard lab strain FO652.

194 To over-express *aho1*$^{+}$, the coding sequence of *SPAC688.03c* was amplified by PCR
195 and cloned into pREP41-*eGFPC* (Craven et al. 1998).

196 To construct plasmids for over-expression of *hop1*$^{+}$ in *Sz. pombe* we cloned PCR
197 products representing genomic or cDNA versions of the *hop1* coding sequence into pJR-41XL
198 (Moreno et al. 2000). During DNA sequencing we found discrepancies with the *hop1* coding
199 sequence prediction on PomBase (https://www.pombase.org/, last accessed 03/06/2017)
200 (see Results section for details). To corroborate this initial finding we also cloned meiotic
201 cDNA clones from two independently constructed strains (UoA399 and UoA722) into pUC8.

202 All plasmid constructs (for sequences see supporting online material, Lorenz 2018),
203 as well as epitope-tagged, splice variant, and *hop1-ΔHORMAD* strains were verified by DNA
204 sequencing (Source BioScience plc, Nottingham, UK).

205 All DNA modifying enzymes (high-fidelity DNA polymerase Q5, restriction
206 endonucleases, T4 DNA ligase) and NEBuilder HiFi DNA Assembly Master Mix were obtained
207 from New England BioLabs. Oligonucleotides were supplied by Sigma-Aldrich Co. (St. Louis,
208 MO, USA).

209

210 **Genetic and molecular biology techniques**

211 Spot assays to monitor growth and genotoxin sensitivities were essentially performed as
212 described previously (Doe et al. 2000; Lorenz et al. 2009). Spot assays of deletion strains
213 were done on YE plates, and of strains harboring plasmids on EMMG plates containing the
214 required supplements. To repress gene expression from pREP41-type plasmids in strains

215 grown on EMMG, thiamine was added to a final concentration of 4 μM (Sabatinos and
216 Forsburg 2010).

217 Genetic recombination assays and spore viability testing by random spore analysis
218 have been described in detail (Osman et al. 2003; Lorenz et al. 2010, 2012, 2014; Sabatinos
219 and Forsburg 2010).

220 Meiotic cDNA was obtained from cells undergoing synchronized azygotic wild-type
221 meiosis. Aliquots of cell culture were drawn at several time-points during a meiotic time-
222 course by first extracting RNA using the NucleoSpin TriPrep kit (Macherey-Nagel GmbH & Co.
223 KG, Düren, Germany) and then reverse-transcribing the RNA into cDNA using the ProtoScript
224 II First Strand cDNA Synthesis kit (New England BioLabs) following the instructions of the
225 respective manufacturer.

226

227 **Chromatin spreads, immunocytochemistry, and microscopy**

228 Nuclear spreads of meiotic *Sz. pombe* cells were prepared as described previously (Loidl and
229 Lorenz 2009), with the only modification that Lallzyme MMX (Lallemand Inc., Montréal,
230 Canada) at a final concentration of 100 mg/ml was used as the sole enzyme in the
231 spheroplasting solution (Flor-Parra et al. 2014).

232 Immunostaining was performed as previously described (Loidl and Lorenz 2009) using
233 polyclonal rabbit α-myc (ab9106; Abcam PLC, Cambridge, UK) at a 1:500 dilution and
234 monoclonal rat α-GFP [3H9] (ChromoTek GmbH, Planegg-Martinsried, Germany) at a 1:100
235 dilution as primary antibodies. Antibody-bound protein was visualized using donkey α-rabbit
236 IgG AlexaFluor-555 (ab150062; Abcam) and donkey α-rat IgG AlexaFluor-488 (ab150153;
237 Abcam), both at a 1:500 dilution, as secondary antibodies conjugated to fluorophores. DNA

238 was stained by Hoechst 33342 (Molecular Probes, Eugene, OR, USA) at a final concentration
239 of 1 μg/ml.
240 Analysis was done using a Zeiss Axio Imager.M2 (Carl Zeiss AG, Oberkochen,
241 Germany) epifluorescence microscope equipped with the appropriate filter sets to detect
242 red, green, and blue fluorescence. Black-and-white images were taken with a Zeiss AxioCam
243 MRm CCD camera controlled by AxioVision 40 software v4.8.2.0. Images were pseudo-
244 coloured and overlayed using Adobe Photoshop CC (Adobe Systems Inc., San José, CA, USA).
245
246 **Data presentation and statistics**
247 Data presented as box-and-whisker plots were created in RStudio 1.0.136 (R version 3.3.1)
248 (http://www.r-project.org/) using the boxplot() function with its standard settings. The lower
249 and upper 'hinges' of the box represent the first and third quartile, respectively, and the
250 black bar within the box indicates the median (=second quartile). The 'whiskers' represent
251 the minimum and maximum of the range, unless they differ more than 1.5-times the
252 interquartile distance from the median. In the latter case, the borders of the 1.5-times
253 interquartile distance around the median are indicated by the 'whiskers' and values outside
254 this range ('outliers') are shown as open circles. Raw data and R scripts used for the
255 boxplot() function are available online as supporting material (Lorenz 2018).
256 Initially, all data involving multiple comparisons underwent an overall statistical
257 assessment using a Kruskal-Wallis one-way analysis of variance to verify that there indeed
258 are statistically significant differences ($\alpha < 0.05$) between data sets within one experiment.
259 All direct one-on-one statistical comparisons between control and experimental data were
260 done using a two-tailed Mann-Whitney U test. Both Kruskal-Wallis and Mann-Whitney U
261 tests are non-parametric and therefore do not assume normal distribution of data points

262 within a data set. Kruskal-Wallis analyses were performed in IBM SPSS Statistics 24.0.0.0
263 (International Business Machines Corporation, Armonk, NY, USA), and Mann-Whitney U tests
264 in G*Power 3.1.9.2 (Faul et al. 2007, 2009). *P* values listed in Supplementary Tables S2 and
265 S3 were determined with a statistical power ($1 - \beta$) set to 0.8.
266

267 **Results**

268 **Correction of the *Sz. pombe hop1* coding sequence**

269 When constructing plasmids to over-express *hop1*$^{+}$ in fission yeast cells, sequencing of our
270 cDNA clones revealed major discrepancies compared to the annotated sequence on
271 PomBase (https://www.pombase.org/, last accessed 03/06/2017). These differences
272 resulted from the incorrect annotation of the position of the third intron (Figs. 1b, S1, S2).
273 Additionally, we detected two splice variants (sv) of *hop1*
274 (https://www.ebi.ac.uk/ena/data/view/LT963776;
275 https://www.ebi.ac.uk/ena/data/view/LT907816). The main cDNA version (*hop1-sv1*)
276 translated into a protein with 527 amino acids (AAs) in length which is one AA shorter than
277 the currently annotated one (528 AAs). The discrepancy affects AAs 138-156/157 in the core
278 region of the HORMA domain (Fig. 1). A second, shorter splice variant (*hop1-sv2*) seems to
279 use a downstream AG as an alternative splice acceptor site at the third intron, thereby
280 expanding it by another 21 bps (Figs. 1b, S1, S2). In a total of 25 cDNA clones from meiotic
281 cDNA preparations of two independently constructed strains drawn from different time-
282 points of a meiotic time-course, 23 were of the *hop1-sv1* type, one conformed to the *hop1-*
283 *sv2* type, and one was aberrant representing a rather short form of *hop1* with a frame-shift
284 (Fig. 1c). Considering the scarcity of *hop1-sv2* in our samples, it could well represent a
285 splicing accident or even a PCR artefact.

286 Using ClustalΩ (Sievers et al. 2014) the translation of the experimentally determined
287 Hop1-sv1 HORMA domain sequence also produces a slightly better alignments with Hop1
288 HORMA domains of other *Schizosaccharomyces* (Fig. S3) species than the predicted one. The
289 region of discrepancy in the experimentally derived *Sz. pombe* Hop1 HORMA domain
290 (VCKFFNRLHESFIKLINVQKE) aligns without much gapping (only one AA position in *Sz.*
291 *octosporus* and *Sz. cryophilus* shows a gap) and 7 fully conserved or strongly similar positions
292 to its counterpart in the other *Schizosaccharomyces* species. The same region from the
293 predicted *Sz. pombe* Hop1 (VSYQRSERFVIKLFLSGNVKTE) produces a large gap in the
294 alignment with the *Sz. japonicus* sequence, receives a three AAs gap compared to *Sz.*
295 *octosporus* and *Sz. cryophilus*, and aligns with only 4 fully conserved or strongly similar
296 positions. Over the whole length of the HORMA domain in this multi-species comparison,
297 this results in 10 fully conserved and 34 strongly similar AA residues in the alignment for the
298 predicted *Sz. pombe* Hop1 sequence, and in 11 fully conserved and 35 strongly similar AA
299 residues with the experimentally derived one (Fig. S3). This demonstrates that the current
300 annotation of the *hop1* open reading frame on PomBase (https://www.pombase.org/) is
301 erroneous, and that the long, predominant splice variant (*hop1-sv1*;
302 https://www.ebi.ac.uk/ena/data/view/LT963776) we identified in our cDNA clones is the
303 correct transcript of *hop1*.
304

305 **The long *hop1* splice variant *hop1-sv1* is sufficient for meiotic recombination**

306 We were interested in establishing whether the long, predominant version of Hop1 (Hop1-
307 sv1) is fully functional, and whether solely expressing the rare short version Hop1-sv2
308 (lacking 7 AAs in the HORMA domain, see Fig. 1) causes a phenotype. Additionally, we
309 constructed a Hop1 version which lacks the HORMA domain altogether, Hop1-ΔHORMAD. In

310 *S. cerevisiae* removing the N-terminal 268 AAs of Hop1 – which includes the HORMA domain
311 – has previously been shown to abolish spore viability completely, however the C-terminal
312 fragment remaining is still capable of binding DNA *in vitro* (Khan et al. 2013). In contrast, the
313 *M127K* point mutation in the center of the HORMA domain of *C. elegans HTP-1*, one of four
314 meiotic HORMA-paralogs in the nematode, results in only a minor meiotic phenotype
315 despite HTP-1^{M127K} not localizing to meiotic chromosome axes (Silva et al. 2014). The *Sz.*
316 *pombe* short form *hop1-sv2* is apparently not strongly expressed (if not a splicing accident or
317 PCR artefact) in a wild-type background and thus unlikely to play a (major) role. However, in
318 light of the distinct phenotypes of HORMA-domain mutants in budding yeast and *C. elegans*,
319 we wanted to use the *hop1-sv2* variant and the *hop1-ΔHORMAD* mutant to probe the role of
320 the HORMA domain for meiotic recombination and Hop1 localization to meiotic chromatin in
321 fission yeast. The 7 AAs (positions 157-163) missing in Hop1-sv2 are close to the boundary
322 between the HORMA core domain and the HORMA "safety-belt" region (Fig. 1a, b; Fig. S2)
323 (Rosenberg and Corbett 2015; West et al. 2017), and their loss might affect interaction of
324 Hop1 with the meiotic chromosome axis similar to nematode HTP-1^{M127K} and also interfere
325 with Hop1's self-oligomerization. The *hop1-ΔHORMAD* strains serve as controls, to monitor
326 the effect removal of the complete HORMA domain has on meiotic recombination and Hop1
327 localization.

328 Previously, it has been shown that the full deletion of *hop1* causes a reduction in
329 both intragenic (gene conversion) and intergenic (crossover) recombination at several
330 genetic intervals in fission yeast with a concomitant increase in intrachromosomal
331 recombination (Latypov et al. 2010). The *hop1* deletion also leads to defects in homologous
332 pairing along chromosome I during meiosis (Latypov et al. 2010). These phenotypes can at
333 least be partially explained by a reduction in DSB formation and a preponderance of DSBs

334 being repaired from the sister chromatid rather than the homolog (Rothenberg et al. 2009;
335 Latypov et al. 2010). Using our meiotic recombination assay system (Lorenz et al. 2010)
336 which allows us to concomitantly measure spore viability, and the frequency of gene
337 conversion (GC), crossovers (COs) and COs with GC events we found a statistically significant
338 decrease in all recombination measures in a *hop1*Δ compared to a wild-type cross (Fig. 2).
339 Indeed, GC decreased 4.7-fold ($p = 4.53 \times 10^{-13}$) (Fig. 2b), COs 2.8-fold ($p = 3.61 \times 10^{-6}$) (Fig.
340 2c), and COs associated with GC events were reduced by 8.7 percentage points ($p = 0.01$)
341 (Fig. 2d) (see also Table S2). Overall, this reduction in recombination outcome did not
342 negatively affect spore viability (Table S2). Recombination of a strain expressing only the
343 long, predominant version *hop1-sv1* (from the *hop1*-promoter at its original locus without
344 any marker genes inserted) was indistinguishable from wild type, whereas replacing the
345 wild-type copy of *hop1* with *hop1-sv2* led to a moderate reduction in GC (1.4-fold, $p = 1.51 \times$
346 10^{-3}) and COs (1.7-fold, $p = 2.27 \times 10^{-3}$), but not in COs associated with GC events ($p = 0.76$)
347 compared to wild type (Fig. 2, Table S2). The *hop1-ΔHORMAD* in turn was indistinguishable
348 from a full deletion (Fig. 2, Table S2). These results indicate that in line with *hop1-sv1* being
349 the predominant, if not the exclusive, splice variant behaves like wild-type *hop1* containing
350 all its introns, that *hop1-sv2* lacking 21 nucleotides in the HORMA domain is not fully
351 functional producing a hypomorphic phenotype, and that removal of the complete HORMA
352 domain (*hop1-ΔHORMAD*) produces a null phenotype.
353

354 **Hop1 localizes to meiotic chromatin and forms linear elements independent of a full-**
355 **length HORMA domain**

356 As with organisms possessing a fully-fledged synaptonemal complex, Hop1 localizes to
357 meiotic chromosome axes, called linear elements, in fission yeast (Lorenz et al. 2004).

358 However, the deletion of *hop1* has little impact on linear element formation *per se* (Lorenz
359 et al. 2006). We were keen to understand whether the presence of the HORMA domain is
360 required for localization of Hop1 to linear elements. We used immunostaining on chromatin
361 spreads from meiotic fission yeast cells to detect heterozygously 13myc-tagged Hop1-sv1,
362 Hop-sv2, and Hop1-ΔHORMAD in homozygous *hop1-sv1*, *hop1-sv2*, and *hop1-ΔHORMAD*
363 strains, respectively. Hop1-sv1-13myc formed linear elements, and all four morphological
364 classes of linear elements (dots, threads, networks, and bundles) were observed (Fig. 3a-d)
365 (Bähler et al. 1993; Lorenz et al. 2004, 2006). This result is consistent with the wild-type
366 phenotype for meiotic recombination of *hop1-sv1* crosses. Intriguingly, Hop1-sv2-13myc was
367 indistinguishable from Hop1-sv1-13myc (Fig. 3e-h). Therefore, the loss of the 7 AAs close to
368 the boundary between the HORMA core domain and the HORMA "safety-belt" region in the
369 *hop1-sv2* allele does not conspicuously influence recruitment of Hop1 to linear elements,
370 despite affecting meiotic recombination (Fig. 2b-d). Hop1-ΔHORMAD-13myc could not be
371 detected on meiotic chromatin (Fig. S4) (a GFP-tagged version of the linear element protein
372 Mug20 served as control to identify meiotic nuclei containing linear elements; (Estreicher et
373 al. 2012)), this is consistent with *hop1-ΔHORMAD* displaying a meiotic recombination
374 phenotype similar to *hop1Δ* (Fig. 2b-d).
375
376 **Searching for Hop1 interactors**
377 A bio-informatics screen using the *Pombe* Interactome (PInt) (Pancaldi et al. 2012) for
378 potential Hop1 interactors retrieved *SPAC688.03c* as the highest hit from an uncharacterized
379 open reading frame (10th highest overall). The gene product of *SPAC688.03c* localizes
380 preferentially to the nucleus (Matsuyama et al. 2006) (Fig. S5) and is upregulated at the
381 onset of meiosis (Mata et al. 2002), which is consistent with a potential role in meiotic

382 chromatin metabolism. Notably, a point mutation in the human ortholog of *SPAC688.03c*,
383 *AMMECR1*, is associated with Alport syndrome (A), mental retardation (M), midface
384 hypoplasia (M), and elliptocytosis (E) (Vitelli et al. 1999; Andreoletti et al. 2017). Therefore,
385 we investigated the phenotype of a *SPAC688.03c* (from here on *aho1*, for *AMMECR1-*
386 *homolog*) deletion in vegetative and generative cells.

387 First, *aho1*Δ was assayed for changes in genotoxin sensitivity and meiotic
388 recombination outcome. The wild-type and *aho1*Δ strains exhibited similar levels of
389 resistance to the topoisomerase I-poison camptothecin (CPT), the alkylating agent methyl
390 methanesulfonate (MMS), the ribonucleotide reductase blocker hydroxyurea (HU), and
391 ultraviolet (UV) radiation (Fig. 4a). The deletion of *aho1* in a wild-type or *hop1*Δ background
392 did not affect spore viability (Fig. 4b). The meiotic recombination outcome of an *aho1*Δ
393 single mutant was similar to wild type, and an *aho1*Δ *hop1*Δ double mutant was
394 indistinguishable from a *hop1*Δ single mutant, except for a moderate 1.4-fold reduction in
395 gene conversion (p = 0.034) (Fig. 4c-e, Table S2). These results indicate that under standard
396 laboratory conditions *aho1*$^+$ is not required for DNA damage repair or meiotic
397 recombination. Therefore, Aho1 is not an essential interactor of Hop1 because it does not
398 mirror the phenotype of *hop1*Δ and we did not observe strong genetic interactions with
399 *hop1*Δ.

400 We tested whether over-expression of *aho1*$^+$ might uncover a DNA repair and/or
401 recombination role. The *aho1*$^+$ gene was put under the control of the thiamine-repressible
402 *nmt1*-promoter at the medium pREP41-level and tagged with GFP at its C-terminus. Spot
403 assays and recombination assays were performed after Aho1-GFP over-expression was
404 induced for 24 hours (see also Fig. S5). Cells over-expressing Aho1-GFP did not show
405 increased genotoxin sensitivities compared to cells containing an empty plasmid, cells over-

406 expressing GFP alone, or cells grown in the presence of thiamine (in which expression is not
407 induced) (Fig. 5a, b). Over-expression of Aho1-GFP also did not alter spore viability and
408 meiotic recombination outcome in comparison to GFP over-expression (Fig. 5c-f, Table S3),
409 indicating that a massive surplus of Aho1 protein has no negative impact on reproductive
410 success.
411
412 ***hop1* displays genetic interactions with the structure-selective endonuclease *mus81* and**
413 **the DNA helicase *fml1***
414 Considering that the absence of *hop1* reduces recombination outcome in a similar fashion to
415 Rad51/Dmc1-mediator (*rad55-rad57*, *swi5-sfr1*, and *rlp1-rdl1-sws1*) mutants (Lorenz et al.
416 2012, 2014) (Fig. 2) we were wondering how *hop1* genetically interacts with the key meiotic
417 determinants of CO and non-CO formation, *mus81* and *fml1*.
418 The deletion of *hop1*Δ in a *mus81*Δ background improves spore viability from 1.85%
419 to 18.7% (Fig. 6, Table S2) similar to what has been seen in *mus81*Δ Rad51/Dmc1-mediator
420 double mutants (Lorenz et al. 2010, 2012, 2014). This rescue in spore viability is not
421 accompanied by a restoration of CO frequency. A *hop1*Δ *mus81*Δ mutant shows only 0.2% of
422 COs which is significantly different both from wild type ($p = 1.9 \times 10^{-7}$) and the *hop1*Δ single
423 mutant ($p = 2.7 \times 10^{-3}$) (Fig. 6c, Table S2). Also, the rate of COs associated with GC events at
424 0.71% is significantly lower in the *hop1*Δ *mus81*Δ double mutant than in the wild type
425 (63.0%, $p = 5.3 \times 10^{-12}$) or the *hop1*Δ single mutant (54.3%, $p = 3.4 \times 10^{-15}$) (Fig. 6d, Table S2).
426 Removal of *fml1*$^{+}$ increases COs associated with GC events to 72.2% (~10 percentage
427 points more than wild type) (Lorenz et al. 2012), but has little effect on other recombination
428 outcomes (Fig. 6). In *fml1*Δ *hop1*Δ double mutants, there are 72.6% of COs associated with
429 GC events which is significantly different from both wild type ($p = 3.4 \times 10^{-3}$) and a *hop1*Δ

430 single mutant (p = 4.9 × 10^{-9}), but indistinguishable from a *fml1*Δ single mutant (p = 0.78)
431 (Fig. 6d, Table S2). Overall CO formation is not changed compared to *hop1*Δ (p = 0.78), but
432 significantly different from wild type (p = 7 × 10^{-7}) and *fml1*Δ (p = 6.3 × 10^{-8}) (Fig. 6c, Table
433 S2). Also GC frequency is unchanged compared to *hop1*Δ (p = 0.49) (Fig. 6b, Table S2)
434 suggesting that in the absence of *hop1*$^{+}$ the DNA helicase Fml1 does not gain any additional
435 functionality.
436
437 ***hop1* does not show strong genetic interactions with Rad51/Dmc1-mediator mutants**
438 Rad51/Dmc1-mediators are highly conserved, positive determinants of meiotic
439 recombination (Schwacha and Kleckner 1997; Ellermeier et al. 2004; Hayase et al. 2004;
440 Bleuyard et al. 2005; Hyppa and Smith 2010; Lorenz et al. 2012, 2014; Sasanuma et al. 2013).
441 In fission yeast the meiotic recombination phenotype of the *hop1*Δ crosses strongly
442 resembles that of Rad51/Dmc1-mediator mutants in that it reduces all meiotic
443 recombination outcomes and alleviates the effects of a *mus81*Δ mutants (see above).
444 Therefore, we were interested in how *hop1* genetically interacts with the mediators *sfr1*,
445 *rad55*, and *rlp1*, as well as *dmc1* itself. The deletion of *hop1*$^{+}$ leads to a notable reduction in
446 DSB formation (Rothenberg et al. 2009; Latypov et al. 2010), and some of the decrease in
447 recombination frequency in *hop1*Δ is likely due to low DSB formation. This reduction may be
448 unrelated to Rad51/Dmc1-mediator function, because absence of the Sfr1-cofactor *swi5*$^{+}$ or
449 of *dmc1*$^{+}$ does not appreciably reduce DSB formation (Young et al. 2004). We pose that in
450 the absence of *hop1*$^{+}$, which contributes to the establishment of a meiosis-specific
451 chromatin environment, successful sexual reproduction will become more reliant on the
452 mitotic repair factors Rad55 and Rlp1. Therefore, we expected a substantial negative genetic
453 interaction of *hop1* with *sfr1*, *rad55*, *rlp1*, and *dmc1*.

454 Indeed, *hop1*Δ *rad55*Δ and *hop1*Δ *rlp1*Δ double mutants displayed significantly lower
455 GC ($p = 5.3 \times 10^{-5}$ and $p = 0.02$, respectively) than a *hop1*Δ single mutant; the GC level is also
456 notably lower than in *rad55*Δ ($p = 2.9 \times 10^{-5}$) and *rlp1*Δ ($p = 1.3 \times 10^{-4}$) (Fig. 7a , Table S2)
457 (Lorenz et al. 2014). However, overall CO frequency and COs associated with GC events were
458 not significantly different from *hop1*Δ or *rad55*Δ in *hop1*Δ *rad55*Δ, and from *hop1*Δ or *rlp1*Δ
459 in *hop1*Δ *rlp1*Δ (Fig. 7b, c; Table S2). Deletion of *sfr1*$^{+}$ decreased GC rate by 7.5-fold in a
460 *hop1*Δ background to 0.036% ($p = 1.4 \times 10^{-8}$) which is also significantly lower than the 0.13%
461 ($p = 1 \times 10^{-4}$) found in an *sfr1*Δ single mutant (Fig. 7d, Table S2) (Lorenz et al. 2014). Other
462 recombination outcomes were indistinguishable from *hop1*Δ (Fig. 7e, f; Table S2). The
463 interaction of *hop1*Δ with *dmc1*Δ is completely epistatic (Fig. 7d-f, Table S2). Importantly, no
464 noteworthy decreases of spore viability have been observed in any of the double mutants
465 (Table S2). This stands in contrast to double mutant combinations of Rad51/Dmc1-mediators
466 with each other or with *dmc1*Δ; *dmc1*Δ *rad55*Δ, *dmc1*Δ *rlp1*Δ, *rad55*Δ *sfr1*Δ and *rlp1*Δ *sfr1*Δ
467 display strong synergistic reductions in spore viability (Lorenz et al. 2014). Overall, this
468 suggests that in fission yeast meiosis the absence of *hop1*$^{+}$ does not generate a situation
469 which necessitates the presence of a fully functional recombination machinery to produce
470 viable progeny.
471

472 **Discussion**

473 Here we characterize the genetic interactions of *hop1*, which encodes a meiotic HORMA
474 domain protein, with homologous recombination factors in fission yeast. Meiotic HORMADs
475 are components of the meiosis-specific chromosome axis which promote DSB formation to
476 allow for the efficient pairing of homologous chromosomes. At the same time HORMADs
477 attenuate undesirable recombination between sister chromatids (reviewed in Rosenberg

478 and Corbett 2015). In organisms possessing a synaptonemal complex, HORMADs support its
479 formation, and depending on the organism may mount a checkpoint arrest when DSB repair
480 is not completed or homologous chromosomes are not synapsed (Woltering et al. 2000;
481 Armstrong et al. 2002; Couteau and Zetka 2005; Martinez-Perez and Villeneuve 2005;
482 Carballo et al. 2008; Daniel et al. 2011; Rinaldi et al. 2017). *Sz. pombe* meiosis progresses
483 without the formation of a synaptonemal complex, therefore any roles related to the
484 synaptonemal complex will likely not apply. Indeed, DSB formation is reduced and inter-
485 sister recombination is increased in fission yeast *hop1*Δ (Rothenberg et al. 2009; Latypov et
486 al. 2010). Consistent with DSB reduction, decreased numbers of Rec7-foci (an essential co-
487 factor of Spo11) have been observed when *hop1* was absent (Lorenz et al. 2006). As a result
488 of DSB reduction, meiotic inter-homolog recombination frequencies are lower in *hop1*Δ than
489 in wild type (Latypov et al. 2010) (Fig. 2). Thus, the Hop1 function in promoting DSB
490 formation seems to be conserved in fission yeast. In budding yeast Hop1 also acts
491 downstream of DSB formation in promoting Dmc1-dependent inter-homolog recombination
492 by preventing Dmc1-independent Rad51-driven recombination (Niu et al. 2005; Carballo et
493 al. 2008). The suppression of inter-sister recombination is achieved by Hop1-dependent
494 activation of Mek1 which in turn phosphorylates and deactivates the Rad51-mediator Rad54,
495 and also phosphorylates and activates the meiosis-specific Rad51-inhibitor Hed1 (Tsubouchi
496 and Roeder 2006; Niu et al. 2009; Callender et al. 2016). Together, this regulatory network
497 has specific genetic consequences: (I) meiotic recombination cannot proceed without Dmc1
498 which causes a meiotic arrest resulting in an inability to sporulate, and (II) deleting *hop1* in a
499 *dmc1*Δ background restores spore formation by allowing Rad51-dependent DSB repair (Niu
500 et al. 2005; Carballo et al. 2008). In fission yeast the genetic interaction between *hop1* and
501 *dmc1* looks quite different (Fig. 7) in that it is epistatic, however neither single mutant has as

502 strong a phenotype as the corresponding mutants in *S. cerevisiae* (Hollingsworth and Byers
503 1989; Bishop et al. 1992; Grishchuk and Kohli 2003; Latypov et al. 2010). Two features may
504 account for this apparent difference between the two yeasts: The budding yeast is probably
505 the only organism which shuts down Rad51 strand exchange activity via Hed1 (Tsubouchi
506 and Roeder 2006), and fission yeast employs both Rad51 and Dmc1 in their direct strand
507 exchange capacity (Grishchuk and Kohli 2003). Interestingly, the genetic interaction of
508 meiotic *Hormad* and *dmc1* genes generally does not show much conservation. In *Arabidopsis*
509 mutation of *asy1* or *dmc1* causes a strong reduction or absence of chiasmata, respectively,
510 leading to fertility defects. However, the *asy1 dmc1* double mutant looks like a *dmc1* single
511 mutant (Sanchez-Moran et al. 2007). In the mouse both *Dmc1*$^{-/-}$ and *Hormad1*$^{-/-}$ single
512 mutants undergo meiotic arrest at mid-pachytene, and so does the *Dmc1*$^{-/-}$ *Hormad1*$^{-/-}$
513 double mutant (Daniel et al. 2011), i.e. there is no reciprocal rescue as in *S. cerevisiae hop1*Δ
514 *dmc1*Δ. These disparate observations in various model organisms suggest that the genetic
515 networks controlling DSB repair and CO formation, and how these processes are integrated
516 with chromosome axis organization, have undergone considerable rewiring during evolution.
517 Because fission yeast relies on both Rad51 and Dmc1 to invade a repair template during
518 meiotic DSB repair, we also looked at the genetic interaction of *hop1* with Rad51/Dmc1-
519 mediator mutants. Apart from an additive effect on GC frequency in *hop1*Δ *rad55*Δ, *hop1*Δ
520 *rlp1*Δ, and *hop1*Δ *sfr1*Δ double mutants, which can easily be explained by the early functions
521 of Hop1 (reduced DSB formation and increased inter-sister recombination), other
522 recombination outcomes were not different from the *hop1*Δ single mutant (Fig. 7). This
523 indicates that in a fission yeast *hop1*Δ mutant gamete production does not become more
524 reliant on strand exchange than in a wild-type background.

525 Genetic interaction of *hop1*Δ with *mus81*Δ resembled that of *mus81*Δ combined with
526 mutants affecting strand exchange (Ellermeier et al. 2004; Lorenz et al. 2012, 2014), rescuing
527 *mus81*Δ's spore viability defect without rescuing its CO defect (Fig. 6). This interaction can
528 be explained by Hop1 promoting DSB formation and inter-homolog recombination: Fewer
529 DSBs and fewer inter-homolog events in *hop1*Δ decrease the probability of the production of
530 recombination intermediates requiring the action of Mus81. Additionally, the absence of
531 *hop1* might allow DNA helicases to process recombination intermediates as non-COs more
532 efficiently than in a wild-type background.
533 It is well established that fungal Hop1 localizes to the chromosome axis during meiotic
534 prophase by physically interacting with the linear/lateral element protein Rec10/Red1 in
535 fission and budding yeast, respectively (de los Santos and Hollingsworth 1999; Spirek et al.
536 2010). Considering Hop1's central role in coordinating meiotic progression, it is not unlikely
537 that it would physically interact with previously uncharacterized meiotic players; indeed with
538 IHO1, a novel HORMAD1-interactor has recently been described in mice (Stanzione et al.
539 2016). A bio-informatical protein interaction-predictor PInt (Pancaldi et al. 2012) suggested
540 that the uncharacterized AMMECR1-homolog Aho1 might be a potential Hop1-interactor in
541 fission yeast. However, neither deletion nor over-expression of Aho1 indicates a clear
542 meiotic function, independent of the presence or absence of Hop1 (Figs. 4, 5).
543 One of the determining features of Hop1 is its HORMA domain whose function was
544 enigmatic until recently, when it was implicated in the recruitment of Hop1 to the meiotic
545 chromosome axis and in its self-assembly into larger homomeric complexes (Kim et al. 2014;
546 Rosenberg and Corbett 2015). We exploited a cDNA clone of *hop1* (*hop1-sv2*) which
547 produces a protein that lacks 7 AAs in the HORMA domain and constructed a version of hop1
548 lacking the complete HORMA domain (*hop1-ΔHORMAD*) to examine whether the HORMA

549 domain in fission yeast Hop1 is essential for its function and localization. Interestingly,
550 expressing Hop1-sv2 in place of wild-type Hop1 did not result in a notable reduction in
551 localization to chromatin, however it did cause a hypomorphic phenotype for GC and CO
552 frequency outcome, whereas the complete removal of the HORMA domain from Hop1
553 mimicked a deletion phenotype (Figs. 2, 3, S4). This suggests that the shortened HORMA
554 domain in Hop1-sv2 is still partially functional, because absence of Hop1's HORMA domain in
555 fission yeast completely abolishes localization to meiotic chromatin causing a *hop1*Δ
556 phenotype in recombination outcome.
557 It is very interesting how genetic pathways driving meiotic chromosome organization and
558 meiotic recombination are rewired during evolution. The fission yeast, which is lacking a
559 synaptonemal complex, but retains remnants of a meiosis-specific chromosome axis, is a
560 great model for probing the roles of conserved meiotic factors such as Hop1. Clearly, Hop1
561 fulfills an important meiotic function in promoting DSB formation and inter-homolog
562 recombination in this organism, but lacks regulatory roles in lieu of the synaptonemal
563 complex, which appears crucial in the majority of organisms performing meiosis with a
564 synaptonemal complex.
565

566 **Acknowledgments**

567 We are grateful to Shin-ichiro Hiraga, Franz Klein, Jürg Kohli, Josef Loidl, Walter W. Steiner,
568 Matthew C. Whitby, and the National BioResource Project (NBRP) Japan for providing strains
569 and/or plasmids, and to K.C. Chan, M. Roca, and D. Whyte for technical assistance. Kevin
570 Corbett, Nancy Hollingsworth, Takashi Kubota, and Josef Loidl are thanked for critically
571 reading a previous version of this manuscript. Microscopy was performed at the University
572 of Aberdeen Microscopy & Histology facility (Kevin Mackenzie). This work was supported by

the Biotechnology and Biological Sciences Research Council UK (BBSRC, Doctoral Training Grant BB/F016964/1), and the University of Aberdeen (College of Life Sciences and Medicine Start-up grant to AL).

Author contributions

SDB: unpublished essential reagents (yeast strains, plasmids), acquisition of data, analysis and interpretation of data, revising the manuscript; ODJ: acquisition of data, revising the manuscript; AL: conception and design, unpublished essential reagents (yeast strains, plasmids), acquisition of data, analysis and interpretation of data, drafting and revising the manuscript.

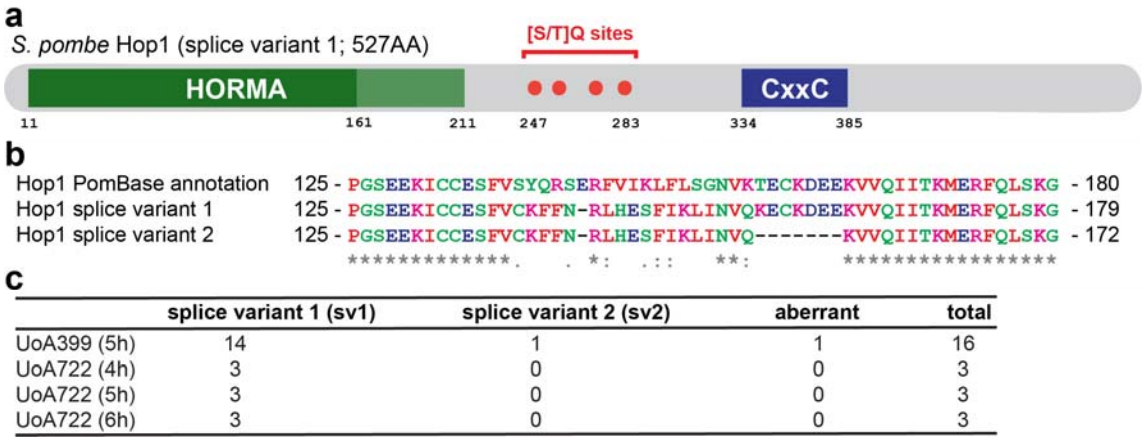

	splice variant 1 (sv1)	splice variant 2 (sv2)	aberrant	total
UoA399 (5h)	14	1	1	16
UoA722 (4h)	3	0	0	3
UoA722 (5h)	3	0	0	3
UoA722 (6h)	3	0	0	3

Figure 1. *Schizosaccharomyces pombe* Hop1 domain structure and alignment between annotated and experimentally determined versions. (**a**) Schematic of the domain structure of the experimentally derived sv1 (splice variant 1) version of Hop1 with the HORMA domain at the N terminus (AAs 11-211), four potential [S/T]Q phosphorylation sites (red dots) distributed between AAs 247 to 283, and residues 334-385 comprising the CxxC Zn-finger domain (dark blue). The HORMA domain can be subdivided into a core domain (dark green) represented by the most C-terminal ~150 AAs and a "safety-belt" region (light green; residues 161-211) (Rosenberg and Corbett 2015; West et al. 2017). Positions of key AA residues are indicated below the schematic. (**b**) ClustalΩ alignment (Sievers et al. 2014) of part of the HORMA domain (starting at residue 125) of the current PomBase-annotation of Hop1, and the two observed splice variants Hop1-sv1 and Hop1-sv2. Colouring of AAs follows the standard ClustalΩ scheme according to physicochemical properties: red for small and small & hydrophobic AAs (AVFPMILW); blue for acidic AAs (DE); magenta for basic AAs (RK); and green for AAs containing hydroxyl-, sulfhydryl-, or amine-groups. Consensus symbols below the alignment indicate full conservation (*) and conservation of groups with strongly similar (:) or weakly similar (.) properties, for details see http://www.ebi.ac.uk/Tools/msa/clustalo/help/faq.html. (**c**) Relative abundance of different *hop1* splice variants found in cDNA of the indicated diploid strains at given time-points of a meiotic time-course.

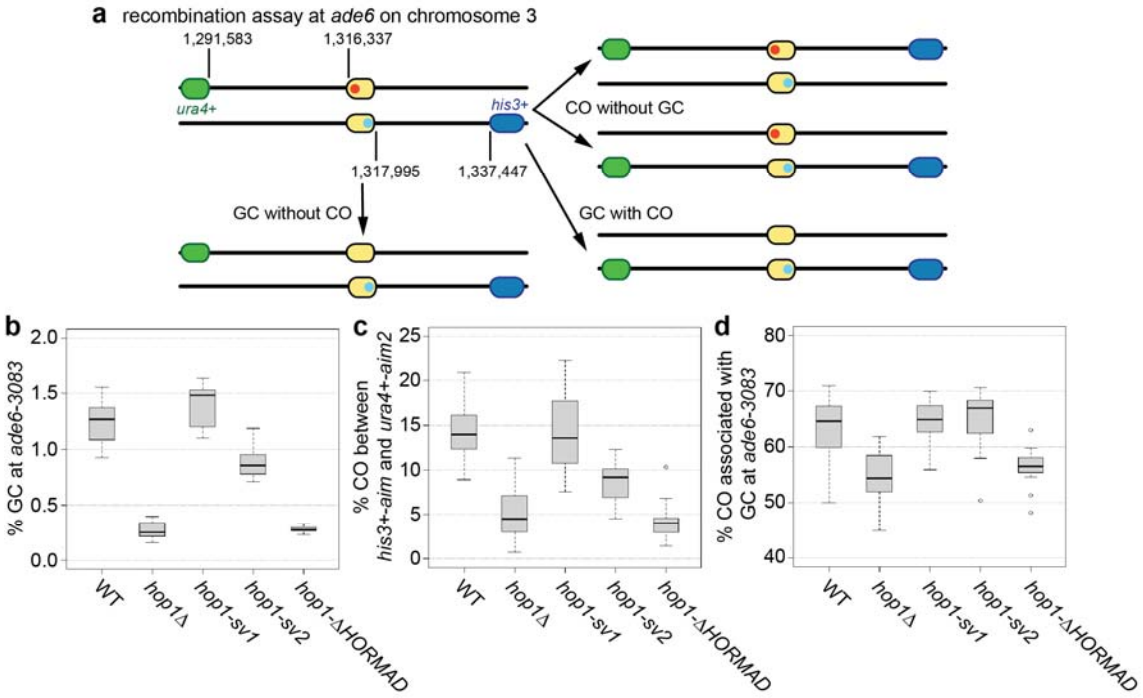

Figure 2. Wild-type and *hop1* mutant levels of meiotic recombination at the *ade6-3083* hotspot. (**a**) Schematic of the recombination assay at *ade6* (yellow) and its prevalent outcomes: positions of *ade6* and the artificially introduced markers *ura4*$^{+}$*-aim2* (green) and *his3*$^{+}$*-aim* (blue) on chromosome III are given in bp; positions of the point mutations in *ade6* in the two parental strains are indicated in red (*ade6-3083*) and light blue (*ade6-469*). (**b**) Frequency of gene conversion (GC) at *ade6-3083*, (**c**) frequency of crossovers (COs) between *ura4*$^{+}$*-aim2* and *his3*$^{+}$*-aim*, and (**d**) percentage of COs between *ura4*$^{+}$*-aim2* and *his3*$^{+}$*-aim* associated with a GC event at *ade6-3083* in crosses of wild type (WT) ALP733×ALP731 (n = 12), *hop1*Δ UoA200×UoA199 (n = 17), *hop1-sv1* UoA766×UoA767 (n = 10), *hop1-sv2* UoA853×UoA854 (n = 12), and *hop1-*Δ*HORMAD* UoA945×UoA944 (n = 12); n indicates the number of independent crosses (see also Table S2).

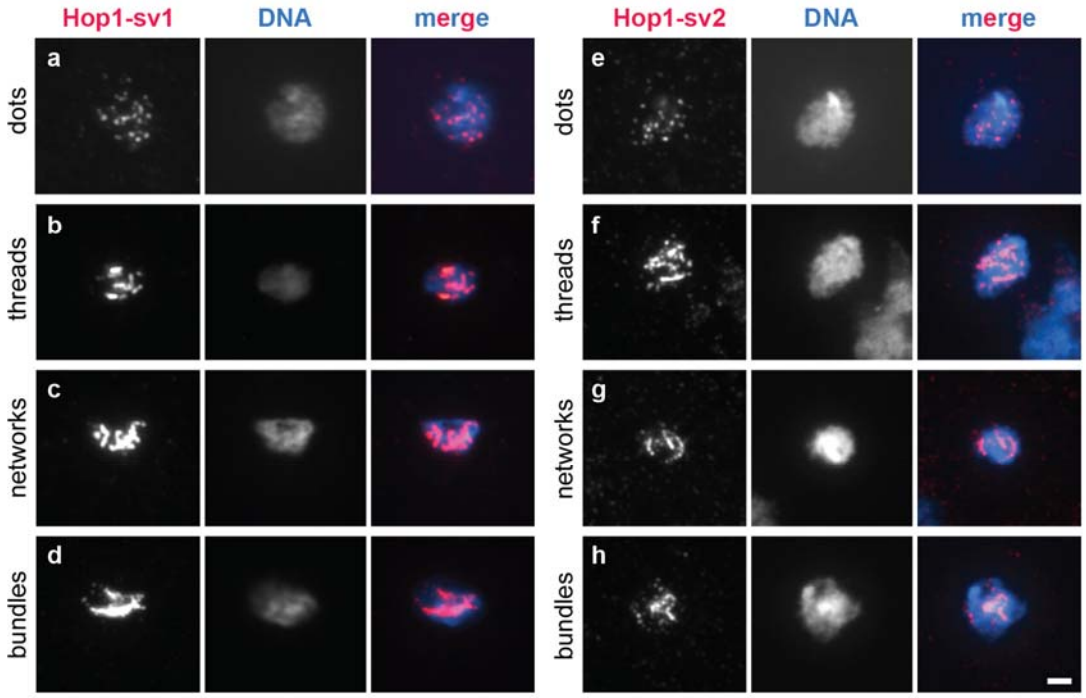

Figure 3. Linear element morphology delineated by immunostaining of Hop1-13myc on chromatin spreads from meiotic fission yeast cells. Linear elements as seen by immunostaining against Hop1-13myc develop from dots via threads to networks and bundles in h^{+N}/h^{-smt0} *hop1-sv1/hop1-sv1::13myc-kanMX6 ade6-M210/ade6-M216* (UoA878) (**a**-**d**) or h^{+N}/h^{-smt0} *hop1-sv2/hop1-sv2::13myc-kanMX6 ade6-M210/ade6-M216* (UoA930) (**e**-**h**). Hop1-13myc is shown in red and Hoechst 33342-stained DNA in blue in the merge panels. Scale bar represents 2 μm.

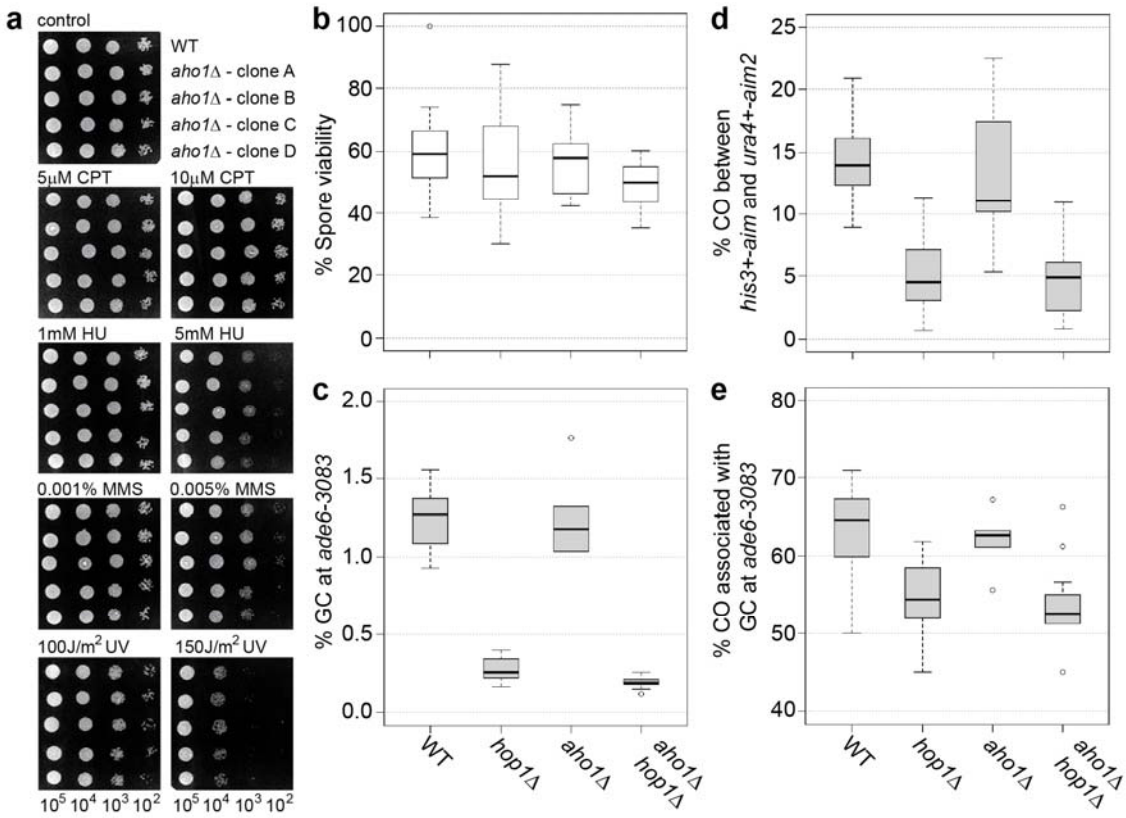

Figure 4. The role of *aho1*$^{+}$ in genotoxic stress resistance and meiotic recombination. (**a**) Spot assays comparing wild type (WT, FO652) and *aho1*Δ (UoA423) for sensitivity to a range of genotoxins; number of cells plated in each spot is indicated at the bottom of the figure. (**b**) Percent spore viability, (**c**) frequency of gene conversion (GC) at *ade6-3083*, (**d**) frequency of crossovers (COs) between *ura4*$^{+}$*-aim2* and *his3*$^{+}$*-aim*, and (**e**) percentage of COs between *ura4*$^{+}$*-aim2* and *his3*$^{+}$*-aim* associated with a GC event at *ade6-3083* in crosses of wild type (WT) ALP733×ALP731 (n = 12), *hop1*Δ UoA200×UoA199 (n = 16), *aho1*Δ UoA424×UoA427 (n = 6), and *aho1*Δ *hop1*Δ UoA785×UoA786 (n = 13); n indicates the number of independent crosses (see also Table S2).

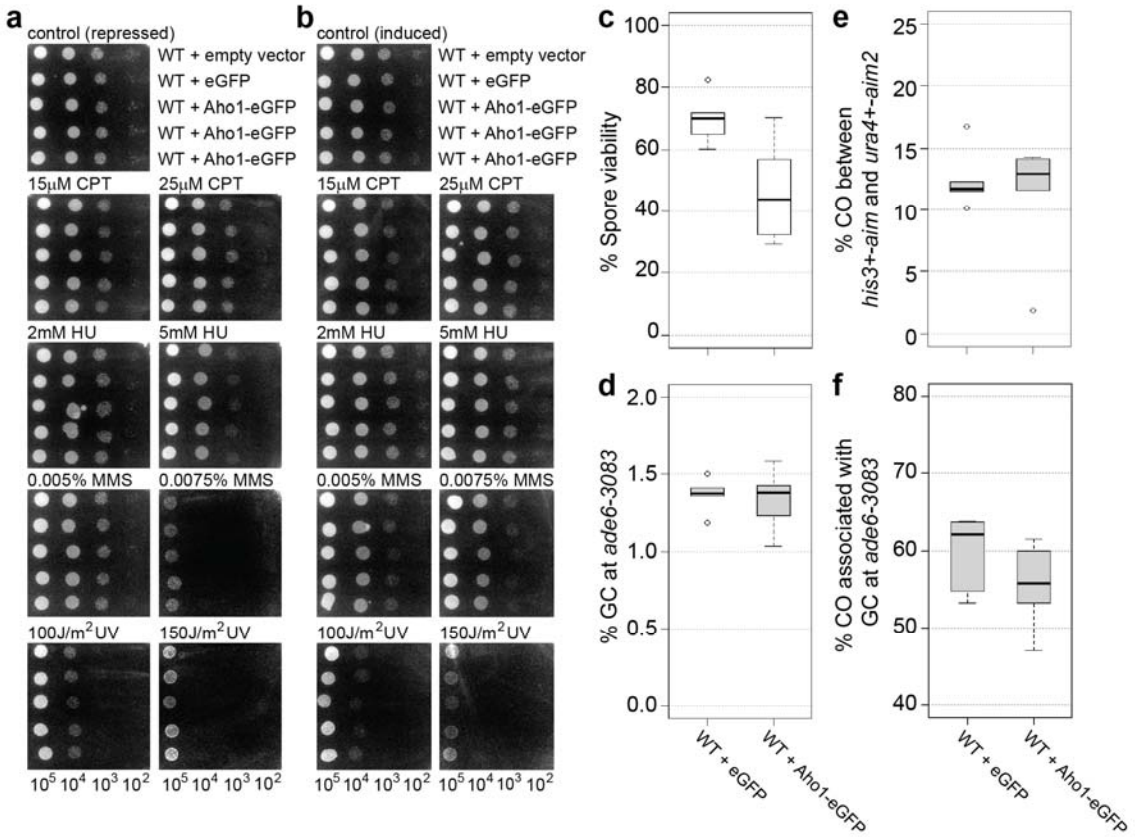

Figure 5. Over-expression of the *aho1*$^{+}$ in wild-type fission yeast cells and its consequences for genotoxic stress resistance and meiotic recombination. (**a**, **b**) Effect of GFP and Aho1-GFP over-expression on the genotoxin sensitivity of wild type (WT, FO652); number of cells plated in each spot is indicated at the bottom of the figure. (**c**) Percent spore viability, (**d**) frequency of gene conversion (GC) at *ade6-3083*, (**e**) frequency of crossovers (COs) between *ura4*$^{+}$*-aim2* and *his3*$^{+}$*-aim*, and (**f**) percentage of COs between *ura4*$^{+}$*-aim2* and *his3*$^{+}$*-aim* associated with a GC event at *ade6-3083* in crosses of wild type (WT) ALP733×UoA841 over-expressing GFP (n = 6), or Aho1-GFP (n = 6); n indicates the number of independent crosses (see also Table S3).

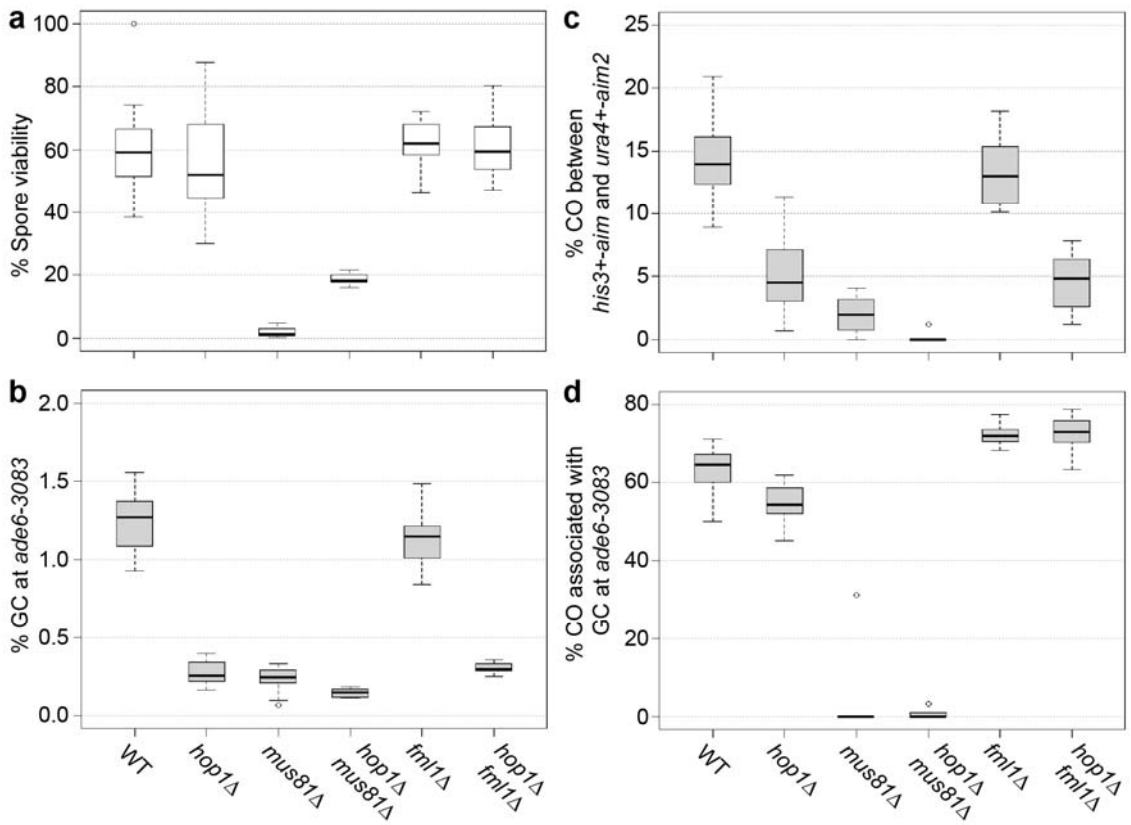

648
649 **Figure 6. Genetic interaction of *hop1*Δ with deletions of factors required for meiotic**
650 **recombination intermediate processing.** (**a**) Percent spore viability, (**b**) frequency of gene
651 conversion (GC) at *ade6-3083*, (**c**) frequency of crossovers (COs) between *ura4*$^{+}$*-aim2* and
652 *his3*$^{+}$*-aim*, and (**d**) percentage of COs between *ura4*$^{+}$*-aim2* and *his3*$^{+}$*-aim* associated with a
653 GC event at *ade6-3083* in crosses of wild type (WT) ALP733×ALP731 (n = 12), *hop1*Δ
654 UoA200×UoA199 (n = 16), *mus81*Δ ALP812×ALP813 (n = 10; in a) and ALP802×ALP822 (n =
655 10; in c-d), *hop1*Δ *mus81*Δ UoA204×UoA203 (n = 6), *fml1*Δ ALP1133×FO2608 (n = 15), and
656 *fml1*Δ *hop1*Δ UoA182×UoA181 (n = 14); n indicates the number of independent crosses (see
657 also Table S2).
658

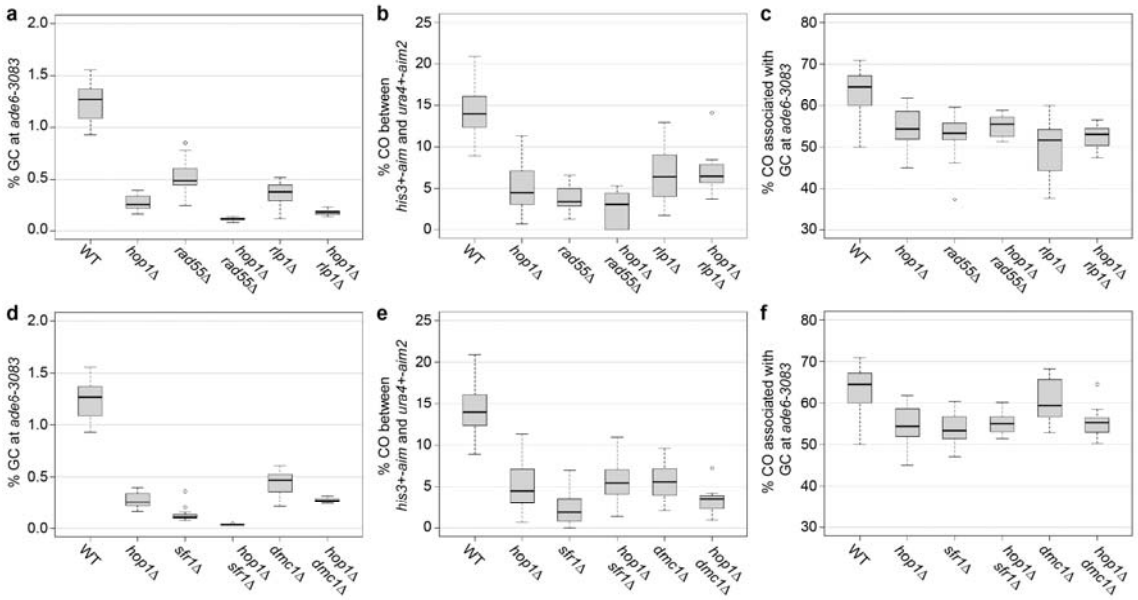

Figure 7. Genetic interaction of *hop1*Δ with deletions of Rad51/Dmc1-mediator genes. (**a**, **d**) frequency of gene conversion (GC) at *ade6-3083*, (**b**, **e**) frequency of crossovers (COs) between *ura4*$^{+}$*-aim2* and *his3*$^{+}$*-aim*, and (**c**,**f**) percentage of COs between *ura4*$^{+}$*-aim2* and *his3*$^{+}$*-aim* associated with a GC event at *ade6-3083* in crosses of wild type (WT) ALP733×ALP731 (n = 12), *hop1*Δ UoA200×UoA199 (n = 16), *rad55*Δ ALP1649×ALP1648 (n = 12), *hop1*Δ *rad55*Δ UoA846×UoA847 (n = 10), *rlp1*Δ ALP1623×ALP1620 (n = 18), *hop1*Δ *rlp1*Δ UoA848×UoA849 (n = 10), *sfr1*Δ ALP800×ALP782 (n = 22), *hop1*Δ *sfr1*Δ UoA844×UoA845 (n = 12), *dmc1*Δ ALP1545×ALP1544 (n = 12), and *dmc1*Δ *hop1*Δ UoA851×UoA852 (n = 10); n indicates the number of independent crosses (see also Table S2).

671 **References**

672 Akamatsu Y, Dziadkowiec D, Ikeguchi M, et al (2003) Two different Swi5-containing protein
673 complexes are involved in mating-type switching and recombination repair in fission
674 yeast. Proc Natl Acad Sci U S A 100:15770–5. doi: 10.1073/pnas.2632890100

675 Andreoletti G, Seaby EG, Dewing JM, et al (2017) *AMMECR1*: a single point mutation causes
676 developmental delay, midface hypoplasia and elliptocytosis. J Med Genet 54:269–277.
677 doi: 10.1136/jmedgenet-2016-104100

678 Aravind L, Koonin E V (1998) The HORMA domain: a common structural denominator in
679 mitotic checkpoints, chromosome synapsis and DNA repair. Trends Biochem Sci 23:284–
680 6. doi: 10.1016/S0968-0004(98)01257-2

681 Armstrong SJ, Caryl AP, Jones GH, Franklin FCH (2002) Asy1, a protein required for meiotic
682 chromosome synapsis, localizes to axis-associated chromatin in *Arabidopsis* and
683 *Brassica*. J Cell Sci 115:3645–55. doi: 10.1242/jcs.00048

684 Bähler J, Wu JQ, Longtine MS, et al (1998) Heterologous modules for efficient and versatile
685 PCR-based gene targeting in *Schizosaccharomyces pombe*. Yeast 14:943–51. doi:
686 10.1002/(SICI)1097-0061(199807)14:10<943::AID-YEA292>3.0.CO;2-Y

687 Bähler J, Wyler T, Loidl J, Kohli J (1993) Unusual nuclear structures in meiotic prophase of
688 fission yeast: a cytological analysis. J Cell Biol 121:241–56. doi: 10.1083/jcb.121.2.241

689 Bishop DK, Park D, Xu L, Kleckner N (1992) *DMC1*: a meiosis-specific yeast homolog of E. coli
690 *recA* required for recombination, synaptonemal complex formation, and cell cycle
691 progression. Cell 69:439–56. doi: 10.1016/0092-8674(92)90446-J

692 Bleuyard J-Y, Gallego ME, Savigny F, White CI (2005) Differing requirements for the
693 Arabidopsis Rad51 paralogs in meiosis and DNA repair. Plant J 41:533–45. doi:
694 10.1111/j.1365-313X.2004.02318.x

695 Brown MS, Bishop DK (2014) DNA strand exchange and RecA homologs. Cold Spring Harb
696 Perspect Biol 7:a016659. doi: 10.1101/cshperspect.a016659

697 Brown SD, Lorenz A (2016) Single-step marker switching in *Schizosaccharomyces pombe*
698 using a lithium acetate transformation protocol. Bio-protocol 6:e2075. doi:
699 10.21769/BioProtoc.2075

700 Cahoon CK, Hawley RS (2016) Regulating the construction and demolition of the
701 synaptonemal complex. Nat Struct Mol Biol 23:369–377. doi: 10.1038/nsmb.3208

702 Callender TL, Laureau R, Wan L, et al (2016) Mek1 down regulates Rad51 activity during
703 yeast meiosis by phosphorylation of Hed1. PLoS Genet 12:e1006226. doi:
704 10.1371/journal.pgen.1006226

705 Carballo JA, Johnson AL, Sedgwick SG, Cha RS (2008) Phosphorylation of the axial element
706 protein Hop1 by Mec1/Tel1 ensures meiotic interhomolog recombination. Cell
707 132:758–70. doi: 10.1016/j.cell.2008.01.035

708 Caryl AP, Armstrong SJ, Jones GH, Franklin FC (2000) A homologue of the yeast *HOP1* gene is
709 inactivated in the *Arabidopsis* meiotic mutant *asy1*. Chromosoma 109:62–71. doi:
710 10.1007/s004120050413

711 Couteau F, Zetka M (2005) HTP-1 coordinates synaptonemal complex assembly with
712 homolog alignment during meiosis in *C. elegans*. Genes Dev 19:2744–56. doi:

713 10.1101/gad.1348205

714 Craven RA, Griffiths DJ, Sheldrick KS, et al (1998) Vectors for the expression of tagged
715 proteins in *Schizosaccharomyces pombe*. Gene 221:59–68. doi: 10.1016/S0378-
716 1119(98)00434-X

717 Daniel K, Lange J, Hached K, et al (2011) Meiotic homologue alignment and its quality
718 surveillance are controlled by mouse HORMAD1. Nat Cell Biol 13:599–610. doi:
719 10.1038/ncb2213

720 de los Santos T, Hollingsworth NM (1999) Red1p, a *MEK1*-dependent phosphoprotein that
721 physically interacts with Hop1p during meiosis in yeast. J Biol Chem 274:1783–90. doi:
722 10.1074/jbc.274.3.1783

723 Ding DQ, Haraguchi T, Hiraoka Y (2016) A cohesin-based structural platform supporting
724 homologous chromosome pairing in meiosis. Curr Genet 62:499–502. doi:
725 10.1007/s00294-016-0570-x

726 Doe CL, Dixon J, Osman F, Whitby MC (2000) Partial suppression of the fission yeast *rqh1*(-)
727 phenotype by expression of a bacterial Holliday junction resolvase. EMBO J 19:2751–62.
728 doi: 10.1093/emboj/19.11.2751

729 Ellermeier C, Schmidt H, Smith GR (2004) Swi5 acts in meiotic DNA joint molecule formation
730 in *Schizosaccharomyces pombe*. Genetics 168:1891–8. doi:
731 10.1534/genetics.104.034280

732 Estreicher A, Lorenz A, Loidl J (2012) Mug20, a novel protein associated with linear elements
733 in fission yeast meiosis. Curr Genet 58:119–27. doi: 10.1007/s00294-012-0369-3

734 Faul F, Erdfelder E, Buchner A, Lang A-G (2009) Statistical power analyses using G*Power 3.1:
735 tests for correlation and regression analyses. Behav Res Methods 41:1149–60. doi:
736 10.3758/BRM.41.4.1149

737 Faul F, Erdfelder E, Lang A-G, Buchner A (2007) G*Power: A flexible statistical power analysis
738 program for the social, behavioral, and biomedical sciences. Behav Res Methods
739 39:175–191. doi: 10.3758/BF03193146

740 Flor-Parra I, Zhurinsky J, Bernal M, et al (2014) A Lallzyme MMX-based rapid method for
741 fission yeast protoplast preparation. Yeast 31:61–6. doi: 10.1002/yea.2994

742 Fukuda T, Daniel K, Wojtasz L, et al (2010) A novel mammalian HORMA domain-containing
743 protein, HORMAD1, preferentially associates with unsynapsed meiotic chromosomes.
744 Exp Cell Res 316:158–71. doi: 10.1016/j.yexcr.2009.08.007

745 Goldstein AL, McCusker JH (1999) Three new dominant drug resistance cassettes for gene
746 disruption in *Saccharomyces cerevisiae*. Yeast 15:1541–53. doi: 10.1002/(SICI)1097-
747 0061(199910)15:14<1541::AID-YEA476>3.0.CO;2-K

748 Goodyer W, Kaitna S, Couteau F, et al (2008) HTP-3 links DSB formation with homolog
749 pairing and crossing over during *C. elegans* meiosis. Dev Cell 14:263–74. doi:
750 10.1016/j.devcel.2007.11.016

751 Gray S, Cohen PE (2016) Control of meiotic crossovers: From double-strand break formation
752 to designation. Annu Rev Genet 50:175–210. doi: 10.1146/annurev-genet-120215-
753 035111

754 Grimm C, Kohli J, Murray J, Maundrell K (1988) Genetic engineering of *Schizosaccharomyces*

755 *pombe*: a system for gene disruption and replacement using the *ura4* gene as a
756 selectable marker. Mol Gen Genet 215:81–6. doi: doi.org/10.1007/BF00331307

757 Grishchuk AL, Kohli J (2003) Five RecA-like proteins of *Schizosaccharomyces pombe* are
758 involved in meiotic recombination. Genetics 165:1031–43.

759 Hartsuiker E, Neale MJ, Carr AM (2009) Distinct requirements for the Rad32(Mre11)
760 nuclease and Ctp1(CtIP) in the removal of covalently bound topoisomerase I and II from
761 DNA. Mol Cell 33:117–23. doi: 10.1016/j.molcel.2008.11.021

762 Haruta N, Kurokawa Y, Murayama Y, et al (2006) The Swi5-Sfr1 complex stimulates
763 Rhp51/Rad51- and Dmc1-mediated DNA strand exchange in vitro. Nat Struct Mol Biol
764 13:823–30. doi: 10.1038/nsmb1136

765 Hayase A, Takagi M, Miyazaki T, et al (2004) A protein complex containing Mei5 and Sae3
766 promotes the assembly of the meiosis-specific RecA homolog Dmc1. Cell 119:927–40.
767 doi: 10.1016/j.cell.2004.10.031

768 Hollingsworth NM, Byers B (1989) *HOP1*: a yeast meiotic pairing gene. Genetics 121:445–62.

769 Hollingsworth NM, Goetsch L, Byers B (1990) The *HOP1* gene encodes a meiosis-specific
770 component of yeast chromosomes. Cell 61:73–84. doi: 10.1016/0092-8674(90)90216-2

771 Hong S, Sung Y, Yu M, et al (2013) The logic and mechanism of homologous recombination
772 partner choice. Mol Cell 51:440–453. doi: 10.1016/j.molcel.2013.08.008

773 Hunter N (2015) Meiotic recombination: the essence of heredity. Cold Spring Harb Perspect
774 Biol 7:a016618. doi: 10.1101/cshperspect.a016618

775 Hyppa RW, Smith GR (2010) Crossover invariance determined by partner choice for meiotic
776 DNA break repair. Cell 142:243–55. doi: 10.1016/j.cell.2010.05.041

777 Iwasaki O, Noma K (2016) Condensin-mediated chromosome organization in fission yeast.
778 Curr Genet 62:739–743. doi: 10.1007/s00294-016-0601-7

779 Keeney JB, Boeke JD (1994) Efficient targeted integration at *leu1-32* and *ura4-294* in
780 *Schizosaccharomyces pombe*. Genetics 136:849–56.

781 Khan K, Madhavan TPV, Kshirsagar R, et al (2013) N-terminal disordered domain of
782 *Saccharomyces cerevisiae* Hop1 protein is dispensable for DNA binding, bridging, and
783 synapsis of double-stranded DNA molecules but is necessary for spore formation.
784 Biochemistry 52:5265–79. doi: 10.1021/bi4005528

785 Kim Y, Rosenberg SC, Kugel CL, et al (2014) The chromosome axis controls meiotic events
786 through a hierarchical assembly of HORMA domain proteins. Dev Cell 31:487–502. doi:
787 10.1016/j.devcel.2014.09.013

788 Kogo H, Tsutsumi M, Ohye T, et al (2012) HORMAD1-dependent checkpoint/surveillance
789 mechanism eliminates asynaptic oocytes. Genes to Cells 17:439–54. doi:
790 10.1111/j.1365-2443.2012.01600.x

791 Lam I, Keeney S (2015) Mechanism and regulation of meiotic recombination initiation. Cold
792 Spring Harb Perspect Biol 7:a016634. doi: 10.1101/cshperspect.a016634

793 Latypov V, Rothenberg M, Lorenz A, et al (2010) Roles of Hop1 and Mek1 in meiotic
794 chromosome pairing and recombination partner choice in *Schizosaccharomyces pombe*.
795 Mol Cell Biol 30:1570–81. doi: 10.1128/MCB.00919-09

796 Loidl J (2016) Conservation and variability of meiosis across the eukaryotes. Annu Rev Genet
797 50:293–316. doi: 10.1146/annurev-genet-120215-035100

798 Loidl J (2006) *S. pombe* linear elements: the modest cousins of synaptonemal complexes.
799 Chromosoma 115:260–71. doi: 10.1007/s00412-006-0047-7

800 Loidl J, Klein F, Scherthan H (1994) Homologous pairing is reduced but not abolished in
801 asynaptic mutants of yeast. J Cell Biol 125:1191–200. doi: 10.1083/jcb.125.6.1191

802 Loidl J, Lorenz A (2009) Analysis of *Schizosaccharomyces pombe* meiosis by nuclear
803 spreading. Methods Mol Biol 558:15–36. doi: 10.1007/978-1-60761-103-5_2

804 Lorenz A (2017) Modulation of meiotic homologous recombination by DNA helicases. Yeast
805 34:195–203. doi: 10.1002/yea.3227

806 Lorenz A (2015) New cassettes for single-step drug resistance and prototrophic marker
807 switching in fission yeast. Yeast 32:703–710. doi: 10.1002/yea.3097

808 Lorenz A (2018) Supporting Online Material - Genetic interactions between the chromosome
809 axis-associated protein Hop1 and homologous recombination determinants in
810 Schizosaccharomyces pombe. doi: 10.6084/m9.figshare.5373163.v2

811 Lorenz A, Estreicher A, Kohli J, Loidl J (2006) Meiotic recombination proteins localize to linear
812 elements in *Schizosaccharomyces pombe*. Chromosoma 115:330–40. doi:
813 10.1007/s00412-006-0053-9

814 Lorenz A, Mehats A, Osman F, Whitby MC (2014) Rad51/Dmc1 paralogs and mediators
815 oppose DNA helicases to limit hybrid DNA formation and promote crossovers during
816 meiotic recombination. Nucleic Acids Res 42:13723–13735. doi: 10.1093/nar/gku1219

817 Lorenz A, Osman F, Folkyte V, et al (2009) Fbh1 limits Rad51-dependent recombination at
818 blocked replication forks. Mol Cell Biol 29:4742–56. doi: 10.1128/MCB.00471-09

819 Lorenz A, Osman F, Sun W, et al (2012) The fission yeast FANCM ortholog directs non-
820 crossover recombination during meiosis. Science 336:1585–8. doi:
821 10.1126/science.1220111

822 Lorenz A, Wells JL, Pryce DW, et al (2004) *S. pombe* meiotic linear elements contain proteins
823 related to synaptonemal complex components. J Cell Sci 117:3343–51. doi:
824 10.1242/jcs.01203

825 Lorenz A, West SC, Whitby MC (2010) The human Holliday junction resolvase GEN1 rescues
826 the meiotic phenotype of a *Schizosaccharomyces pombe mus81* mutant. Nucleic Acids
827 Res 38:1866–73. doi: 10.1093/nar/gkp1179

828 Martín V, Chahwan C, Gao H, et al (2006) Sws1 is a conserved regulator of homologous
829 recombination in eukaryotic cells. EMBO J 25:2564–74. doi: 10.1038/sj.emboj.7601141

830 Martinez-Perez E, Villeneuve AM (2005) HTP-1-dependent constraints coordinate homolog
831 pairing and synapsis and promote chiasma formation during *C. elegans* meiosis. Genes
832 Dev 19:2727–43. doi: 10.1101/gad.1338505

833 Mata J, Lyne R, Burns G, Bähler J (2002) The transcriptional program of meiosis and
834 sporulation in fission yeast. Nat Genet 32:143–7. doi: 10.1038/ng951

835 Matsuyama A, Arai R, Yashiroda Y, et al (2006) ORFeome cloning and global analysis of
836 protein localization in the fission yeast *Schizosaccharomyces pombe*. Nat Biotechnol
837 24:841–7. doi: 10.1038/nbt1222

838 Mimitou EP, Symington LS (2011) DNA end resection-Unraveling the tail. DNA Repair (Amst)
839 10:344–348. doi: 10.1016/j.dnarep.2010.12.004

840 Molnar M (2003) Linear element formation and their role in meiotic sister chromatid
841 cohesion and chromosome pairing. J Cell Sci 116:1719–1731. doi: 10.1242/jcs.00387

842 Moreno MB, Durán A, Ribas JC (2000) A family of multifunctional thiamine-repressible
843 expression vectors for fission yeast. Yeast 16:861–72. doi: 10.1002/1097-
844 0061(20000630)16:9<861::AID-YEA577>3.0.CO;2-9

845 Neale MJ, Pan J, Keeney S (2005) Endonucleolytic processing of covalent protein-linked DNA
846 double-strand breaks. Nature 436:1053–7. doi: 10.1038/nature03872

847 Niu H, Wan L, Baumgartner B, et al (2005) Partner choice during meiosis is regulated by
848 Hop1-promoted dimerization of Mek1. Mol Biol Cell 16:5804–18. doi:
849 10.1091/mbc.E05-05-0465

850 Niu H, Wan L, Busygina V, et al (2009) Regulation of meiotic recombination via Mek1-
851 mediated Rad54 phosphorylation. Mol Cell 36:393–404. doi:
852 10.1016/j.molcel.2009.09.029

853 Olson LW, Eden U, Egel-Mitani M, Egel R (1978) Asynaptic meiosis in fission yeast? Hereditas
854 89:189–199. doi: 10.1111/j.1601-5223.1978.tb01275.x

855 Osman F, Dixon J, Doe CL, Whitby MC (2003) Generating crossovers by resolution of nicked
856 Holliday junctions: a role for Mus81-Eme1 in meiosis. Mol Cell 12:761–74. doi:
857 10.1016/S1097-2765(03)00343-5

858 Osman K, Yang J, Roitinger E, et al (2018) Affinity proteomics reveals extensive
859 phosphorylation of the Brassica chromosome axis protein ASY1 and a network of
860 associated proteins at prophase I of meiosis. Plant J 93:17–33. doi: 10.1111/tpj.13752

861 Pancaldi V, Saraç OS, Rallis C, et al (2012) Predicting the fission yeast protein interaction
862 network. G3 (Bethesda) 2:453–67. doi: 10.1534/g3.111.001560

863 Phadnis N, Cipak L, Polakova S, et al (2015) Casein kinase 1 and phosphorylation of cohesin
864 subunit Rec11 (SA3) promote meiotic recombination through linear element formation.
865 PLoS Genet 11:e1005225. doi: 10.1371/journal.pgen.1005225

866 Rinaldi VD, Bolcun-Filas E, Kogo H, et al (2017) The DNA damage checkpoint eliminates
867 mouse oocytes with chromosome synapsis failure. Mol Cell 67:1026–1036. doi:
868 10.1016/j.molcel.2017.07.027

869 Rosenberg SC, Corbett KD (2015) The multifaceted roles of the HORMA domain in cellular
870 signaling. J Cell Biol 211:745–55. doi: 10.1083/jcb.201509076

871 Rothenberg M, Kohli J, Ludin K (2009) Ctp1 and the MRN-complex are required for
872 endonucleolytic Rec12 removal with release of a single class of oligonucleotides in
873 fission yeast. PLoS Genet 5:e1000722. doi: 10.1371/journal.pgen.1000722

874 Sabatinos SA, Forsburg SL (2010) Molecular genetics of *Schizosaccharomyces pombe*.
875 Methods Enzymol 470:759–95. doi: 10.1016/S0076-6879(10)70032-X

876 Sakuno T, Watanabe Y (2015) Phosphorylation of cohesin Rec11/SA3 by Casein Kinase 1
877 promotes homologous recombination by assembling the meiotic chromosome axis. Dev
878 Cell 32:220–230. doi: 10.1016/j.devcel.2014.11.033

879 Sambrook JF, Russell DW (2000) Molecular Cloning: A Laboratory Manual, 3rd edn. Cold

880 Spring Harbor Laboratory Press, Cold Spring Harbor

881 Sanchez-Moran E, Santos J-L, Jones GH, Franklin FCH (2007) ASY1 mediates AtDMC1-
882 dependent interhomolog recombination during meiosis in *Arabidopsis*. Genes Dev
883 21:2220–33. doi: 10.1101/gad.439007

884 Sasanuma H, Tawaramoto MS, Lao JP, et al (2013) A new protein complex promoting the
885 assembly of Rad51 filaments. Nat Commun 4:1676. doi: 10.1038/ncomms2678

886 Sato M, Dhut S, Toda T (2005) New drug-resistant cassettes for gene disruption and epitope
887 tagging in *Schizosaccharomyces pombe*. Yeast 22:583–91. doi: 10.1002/yea.1233

888 Schwacha A, Kleckner N (1997) Interhomolog bias during meiotic recombination: meiotic
889 functions promote a highly differentiated interhomolog-only pathway. Cell 90:1123–35.
890 doi: 10.1016/S0092-8674(00)80378-5

891 Shinohara A, Gasior S, Ogawa T, et al (1997) *Saccharomyces cerevisiae recA* homologues
892 *RAD51* and *DMC1* have both distinct and overlapping roles in meiotic recombination.
893 Genes to Cells 2:615–29. doi: 10.1046/j.1365-2443.1997.1480347.x

894 Sievers F, Wilm A, Dineen D, et al (2014) Fast, scalable generation of high-quality protein
895 multiple sequence alignments using Clustal Omega. Mol Syst Biol 7:539–539. doi:
896 10.1038/msb.2011.75

897 Silva N, Ferrandiz N, Barroso C, et al (2014) The fidelity of synaptonemal complex assembly is
898 regulated by a signaling mechanism that controls early meiotic progression. Dev Cell
899 31:503–511. doi: 10.1016/j.devcel.2014.10.001

900 Smith GR (2009) Genetic analysis of meiotic recombination in *Schizosaccharomyces pombe*.
901 Methods Mol Biol 557:65–76. doi: 10.1007/978-1-59745-527-5_6

902 Smith GR, Boddy MN, Shanahan P, Russell P (2003) Fission yeast Mus81.Eme1 Holliday
903 junction resolvase is required for meiotic crossing over but not for gene conversion.
904 Genetics 165:2289–93.

905 Smith A V, Roeder GS (1997) The yeast Red1 protein localizes to the cores of meiotic
906 chromosomes. J Cell Biol 136:957–67. doi: 10.1083/jcb.136.5.957

907 Spirek M, Estreicher A, Csaszar E, et al (2010) SUMOylation is required for normal
908 development of linear elements and wild-type meiotic recombination in
909 *Schizosaccharomyces pombe*. Chromosoma 119:59–72. doi: 10.1007/s00412-009-0241-
910 5

911 Stanzione M, Baumann M, Papanikos F, et al (2016) Meiotic DNA break formation requires
912 the unsynapsed chromosome axis-binding protein IHO1 (CCDC36) in mice. Nat Cell Biol
913 18:1208–1220. doi: 10.1038/ncb3417

914 Sung P (1997) Yeast Rad55 and Rad57 proteins form a heterodimer that functions with
915 replication protein A to promote DNA strand exchange by Rad51 recombinase. Genes
916 Dev 11:1111–21. doi: 10.1101/gad.11.9.1111

917 Tripathi P, Pal D, Muniyappa K (2007) *Saccharomyces cerevisiae* Hop1 protein zinc finger
918 motif binds to the Holliday junction and distorts the DNA structure: implications for
919 Holliday junction migration. Biochemistry 46:12530–42. doi: 10.1021/bi701078v

920 Tsubouchi H, Roeder GS (2006) Budding yeast Hed1 down-regulates the mitotic
921 recombination machinery when meiotic recombination is impaired. Genes Dev

922 20:1766–75. doi: 10.1101/gad.1422506

923 Tsutsui Y, Khasanov FK, Shinagawa H, et al (2001) Multiple interactions among the
924 components of the recombinational DNA repair system in *Schizosaccharomyces pombe*.
925 Genetics 159:91–105.

926 Vitelli F, Piccini M, Caroli F, et al (1999) Identification and characterization of a highly
927 conserved protein absent in the Alport syndrome (A), mental retardation (M), midface
928 hypoplasia (M), and elliptocytosis (E) contiguous gene deletion syndrome (AMME).
929 Genomics 55:335–40. doi: 10.1006/geno.1998.5666

930 West AMV, Komives EA, Corbett KD (2017) Conformational dynamics of the Hop1 HORMA
931 domain reveal a common mechanism with the spindle checkpoint protein Mad2.
932 Nucleic Acids Res 1–14. doi: 10.1093/nar/gkx1196

933 Woltering D, Baumgartner B, Bagchi S, et al (2000) Meiotic segregation, synapsis, and
934 recombination checkpoint functions require physical interaction between the
935 chromosomal proteins Red1p and Hop1p. Mol Cell Biol 20:6646–58. doi:
936 10.1128/MCB.20.18.6646-6658.2000

937 Young JA, Hyppa RW, Smith GR (2004) Conserved and nonconserved proteins for meiotic
938 DNA breakage and repair in yeasts. Genetics 167:593–605. doi:
939 10.1534/genetics.103.023762

940 Zetka MC, Kawasaki I, Strome S, Müller F (1999) Synapsis and chiasma formation in
941 *Caenorhabditis elegans* require HIM-3, a meiotic chromosome core component that
942 functions in chromosome segregation. Genes Dev 13:2258–2270. doi:
943 10.1101/gad.13.17.2258

944